Available online at www.worldscientificnews.com

World Scientific News

WSN 28 (2016) 72-83 EISSN 2392-2192

The Inverse Reaction Cross Sections for Some Charged Particles Using the Optical Model Parameters

Rasha S. Ahmed

Department of Physiology and Medical Physics, College of Medicine, Al-Nahrain University, Baghdad, Iraq

E-mail address: rasha_ryadh@yahoo.com

ABSTRACT

p $-$nucleus, ${}^{2}_{1}H$ $-$nucleus, ${}^{3}_{1}H$ $-$nucleus, and ${}^{4}_{2}He$ $-$nucleus inverse reaction cross sections have been determined using the optical model potentials in a wide range of target nuclei started from $A = 1$ to $A = 232$ using several incident particle energies (E = 2, 8, 10, 20, and 40 MeV). In this work, a large number of optical model available parameters were used to calculate the inverse reaction cross section and compared to investigate the effect of the mass number and incident particle energy on the inverse reaction cross section. All the calculations were performed using MATHLAB programming language.

***Keywords*:** Optical reaction cross-sections, pre-equilibrium models, neutrons, charged particles

1. INTRODUCTION

The total reaction cross section in the pre-equilibrium exciton model is the inelastic part of the interaction between the particle and the target nucleus which described by the optical potentials and consist of several parameters. One of these parameters is the emission rate which describe the emission of one or more particles during the reaction. The inverse reaction cross section, which depends on the target nucleus mass number and involve the emitted particle as a function of energy, is an important quantity in determining the emission rate and the total reaction cross section and then the equilibrium and pre-equilibrium spectrum. The inverse reaction cross-section is the optical reaction cross-section of the excited residual nucleus with the emitted particle as the projectile.

This is approximated as the optical reaction cross-section between the residual nucleus in its ground state and the emitted particle. Many calculations have been performed by several authors for calculating the inverse reaction cross section. In previous treatments, the inverse reaction cross sections was taken as the geometrical cross section, but the neutron cross section is known to rise with decreasing energy, for this Dostrovsky [1] presented the energy and mass number dependence of neutron capture cross sections and also the variation of the proton cross section with mass number, energy and with the atomic number Z. Feshbach and Weisskopf [2] describe the energy dependence of the nuclear cross section when the incident particle is a neutron. Shapiro [3] calculate the compound nucleus cross section when the incident particle is charged, (proton, deuteron or alpha particle).

Mani [4], Becchetti [5] and Chatterjee [6] estimates the optical reaction cross section for uncharged and charged particles using several global optical potentials in terms of empirical expressions of the cross sections which depend on the mass number and the projectile energy. Kalbach [7] limited the range of validity of the reaction cross section and add additional energy domains. Before summarizing the optical model equations, it should be noticed that they are all given in terms of the laboratory energy of the particle. The energies are always given in units of MeV, lengths in Fermi, and cross sections in millibarns. The formulae are given for a particle of type b incident on a nucleus B, so that the subscripts b and B denote quantities evaluated for these entities. In this work, we adopted several calculations to determine the inverse reaction cross sections $\sigma_b(\varepsilon)$ for formation a compound nucleus when charged particles like p, ${}_{1}^{2}H$, ${}_{1}^{3}H$, and ${}_{2}^{4}He$ incident on a wide range of nuclei started from ${}_{1}^{1}H$ and ends with ${}_{90}^{232}Th$, using the optical model potentials.

2. THEORY

The inverse reaction cross section has different forms depending on Coulomb barrier B_{col} and other energy domains [7]. At very low energies or lower than E_{bmin}, the sub barrier formula can be negative or pass through the minimum then it start to increase so the cross section at these low energies is set to zero. At high energies, the above-barrier formula decreases too rapidly, and the cross sections are replaced by the geometrical cross section. Between the previous two forms there are additional two forms define the inverse reaction cross section given by [7],

$$\sigma_b(\varepsilon) = \begin{cases} 0 & for\ E_{bL} \le E_{bmin} \\ pE_{bL}^2 + \alpha E_{bL} + \beta & for\ E_{bmin} \le E_{bL} < B_{col} \\ \lambda E_{bL} + \mu + \dfrac{\nu}{E_{bL}} & for\ B_{col} \le E_{bL} \le E_{btest} \\ \max\left(\lambda E_{bL} + \mu + \dfrac{\nu}{E_{bL}}, \sigma_g\right) & for E_{btest} < E_{bL} \end{cases} \qquad (1)$$

The parameters $p, \lambda, \mu, \nu, B_{col}$ and E_{btest} are all listed in Table 1 [7]. Table 2 includes the quantities $p_0, p_1, p_2, \mu_0, \mu_1, \nu_0, \nu_1$, and ν_2 which are numerical constants whose specific values depend on the optical model and needed in determining the previous parameters, these quantities are taken from different references [8-11].

The variables α and β are given by

$$\alpha = -2pB_{col} + \lambda - \frac{\nu}{B_{col}^2} \tag{2}$$

$$\beta = pB_{col}^2 + \mu + \frac{2\nu}{B_{col}} \tag{3}$$

and

$$E_{bmin} = \begin{cases} \left(-\alpha + \sqrt{\alpha^2 - 4p\beta}\right)/2p & for\ \alpha^2 - 4p\beta > 0 \\ -\alpha/2p & for\ \alpha^2 - 4p\beta \le 0 \end{cases} \tag{4}$$

The geometrical cross section is given by

$$\sigma_g = \pi[R_B + r_b]^2 \tag{5}$$

where

$$R_B = r_0 A_B^{1/3} \tag{6}$$

The reaction cross-section data have been carried out by various workers resulting in global parameter sets. In this work some of these works have been considered. For protons the potential parameters for Kalbach [7] and Menet [8] has been adopted. The potentials for Kalbach [7] and Schwandt [9] have been used for incident deuteron. We have also included the results for Kalbach [7] and Becchette [10] for incident triton. Finally, for alpha projectiles the parameter-sets used are those of Kalbach [7] and Huizenga [11].

Table 1. The equations used in determining the reaction cross section [1].

variable	For emitted charged particles
B_{col}	$1.44 Z_b Z_B / \left[1.5 A_B^{1/3} + R_b\right]$
E_{btest}	$\sqrt{\nu/\lambda} + 7$
p	$p_0 + p_1/B_{col} + p_2/B_{col}^2$
λ	$\lambda_0 A_B^{\mu_1} + \lambda_1$
μ	$\mu_0 A_B^{\mu_1}$
ν	$A_B^{\mu_1}[\nu_0 + \nu_1 B_{col} + \nu_2 B_{col}^2]$

Table 2. The Parameter needed for calculating the reaction cross sections.

Parameters	R_b	p_0	p_1	p_2	λ_0	λ_1	μ_0	μ_1	ν_0	ν_1	ν_2	r_0	r_b
Proton													
Kalbach [1]	0	15.7	9.65	-310	0.00437	-16.58	244.7	0.503	273	-182	-1.87	1.23 fm	0
Menet [2]	0	16.99	46.13	-1298	0.0795	-11.9	127.8	0.66	306.8	-118.5	0.225	1.23 fm	0
Deuteron													
Kalbach [1]	1.2 fm	0.8	420	-1650	0.0062	-7.54	583.5	0.337	422	-474	-3.59	1.12 fm	0.8 fm
Schwandt [3]	1.2 fm	-43.73	934.1	-2518	-0.0762	-8.83	337.5	0.49	417.5	-353	5.515	1.12 fm	0.8 fm
Triton													
Kalbach [1]	1.2 fm	-21.4	485	-1610	0.0186	-8.9	686.3	0.325	369	-522	-5	1.12 fm	0.8 fm
Becchette [4]	1.2 fm	-11.04	619.1	-2147	-0.0426	-10.33	601.9	0.37	583	-546.2	1.718	1.12 fm	0.8 fm
Alpha particle $^{4}_{2}He$													

Kalbach [1]	1.2 fm	10.95	-85.2	1150	0.0643	-14	781.2	0.29	-305	-470	-8.58	1.12 fm	1.2 fm
Huizenga [5]	1.2 fm	10.95	-85.2	1146	0.0643	-13.96	781.2	0.29	-304.7	-470	-8.58	1.12 fm	1.2 fm

3. RESULTS, DISCUSSION AND CONCLUSIONS

Using the 10 parameters illustrated in table 2, started from P_0 through ν_2, the optical cross-sections $\sigma_b(\varepsilon)$ for various global parameter sets for the projectiles, p, ${}^2_1H$, ${}^3_1H$, and ${}^4_2He$ were determined. Using these parameters and the equations in Table 1, the mass number and energy dependence of $\sigma_b(\varepsilon)$ is illustrated in Figures (1, 2, 3, and 4) for p, ${}^2_1H$, ${}^3_1H$, and ${}^4_2He$ sequentially below. $\sigma_b(\varepsilon)$ predicts unphysical or negative values when the incident particle energy is small or less than E_{bmin}, for this, $\sigma_b(\varepsilon)$ should be set to zero in this domain. A detailed comparison of the Menet cross-sections σ_p [8] and the earlier parameterization of Kalbach [7] σ_p cross-section, with the dependence on Z, A, and projectile energy is shown in Figure (1). The same procedure is made in figures (2, 3, and 4) using the values correspond to the optical potentials of Schwandt [9] for deuteron, Becchette [5] for triton, and Huizenga [11] for alpha particle.

In all figures the behavior of the cross section is the same, it is start to rise form a certain value and reach its maximum value and then it is drop down to zero. The comparison between the results of Kalbach and others in Figures (1, 2, 3, and 4) when the incident particle energy is 2, 8, 10, 20 and 40 MeV, gives the same behavior but a quite different values, or in other words a different maximum or minimum values of $\sigma_b(\varepsilon)$.

The reason for differences in these values is due to the additional corrections added by Kalbach for the previous results for proton and for complex particles. The proton total reaction cross sections needed to be renormalized in certain mass regions in order to better reproduce experimental total non-elastic cross sections. In addition to the renormalization factors, the sub-barrier for proton and other charged particles was also adjusted. This adjustment was made due to the foundation of too much proton evaporation at the peak of the distribution, while the calculated emission spectrum did not extend to sufficiently low emission energies. This was also corrected by adjusting the parameter p_2.

After illustrating the differences in the earlier results for the inverse reaction cross section and the previously calculated ones, the results for the most resent calculations were indicated in Figure (5). The figure shows the inverse reaction cross section as a function of Z and A. In each figure the curves are now indicate the cross sections for charged particles p, ${}^2_2H$, ${}^3_2H$, and ${}^4_2He$ with the same incident energy. In case of incident alpha particle, the cross section drop down to zero at a law target nucleus mass number, actually lower than that for incident p, ${}^2_2H$, ${}^3_1H$. This is due to the effect of Coulomb barrier potential.

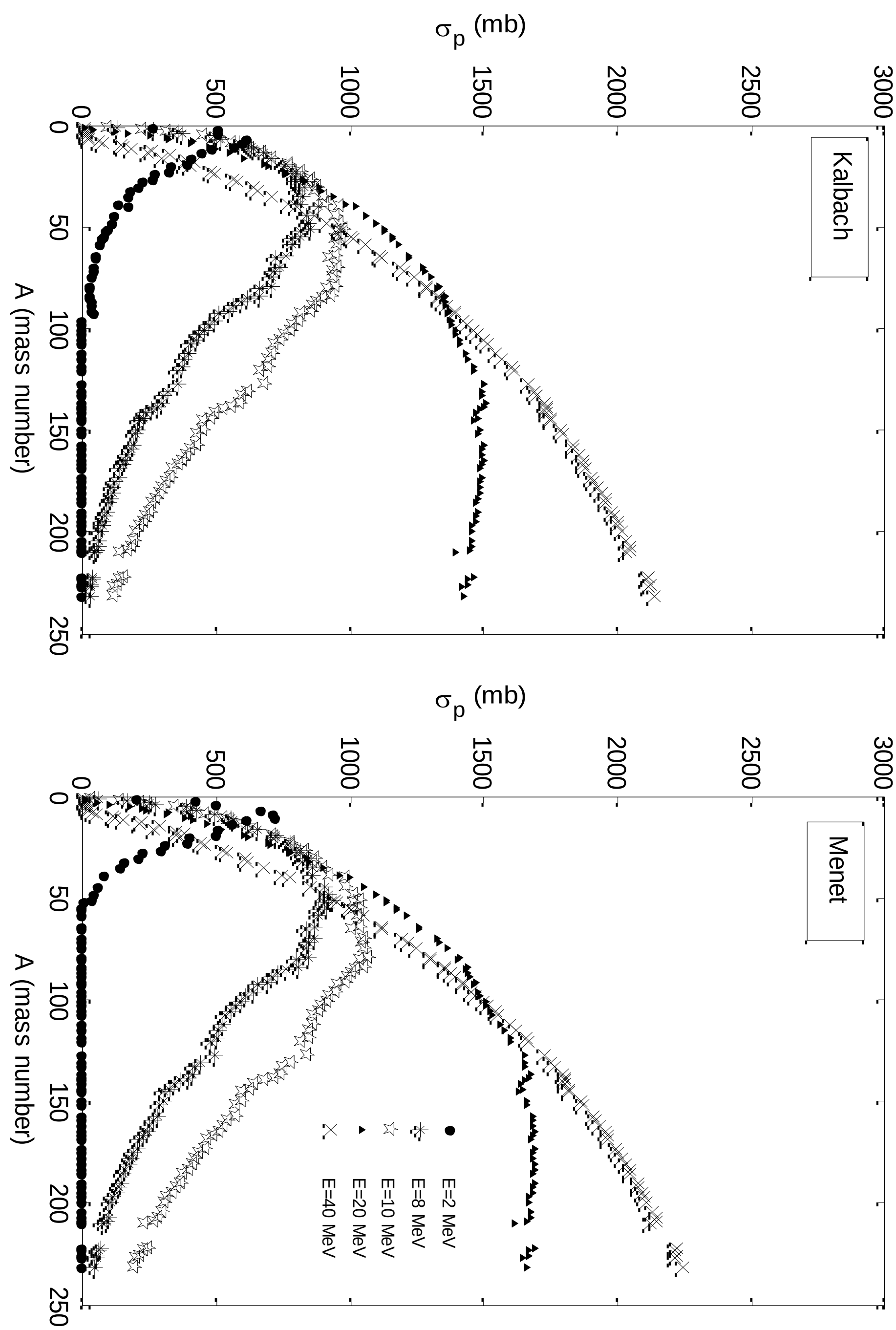

Figure 1. Comparison of the proton optical reaction cross-sections as a function of target mass A, using the global potentials of Kalbach [7] and Menet [8] in different values of the incident particle energy starting from 2 MeV to 40 MeV.

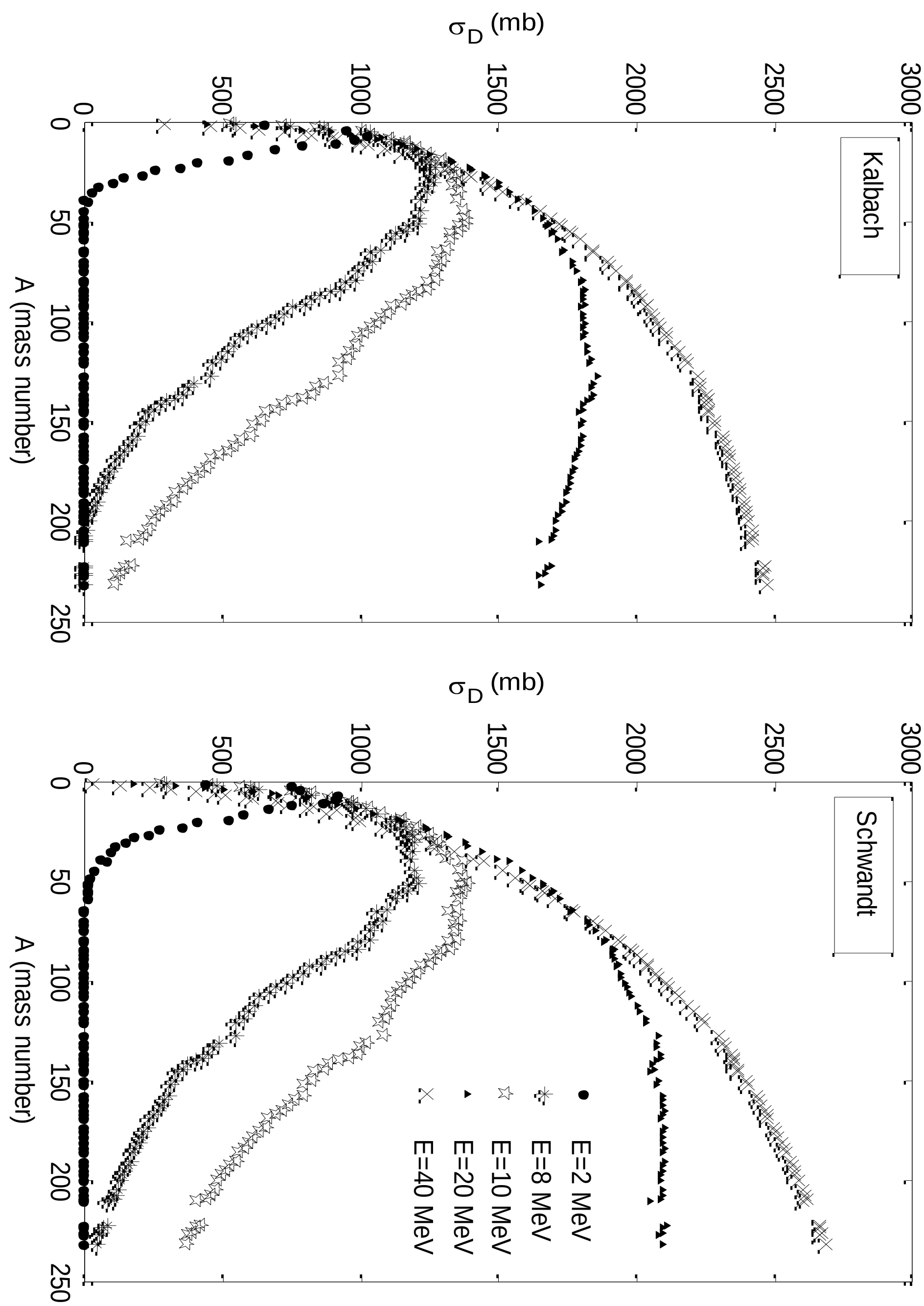

Figure 2. Same as Figure 1 but for incident deuteron and the optical potentials of Kalbach [7] and Schwandt [9] were used.

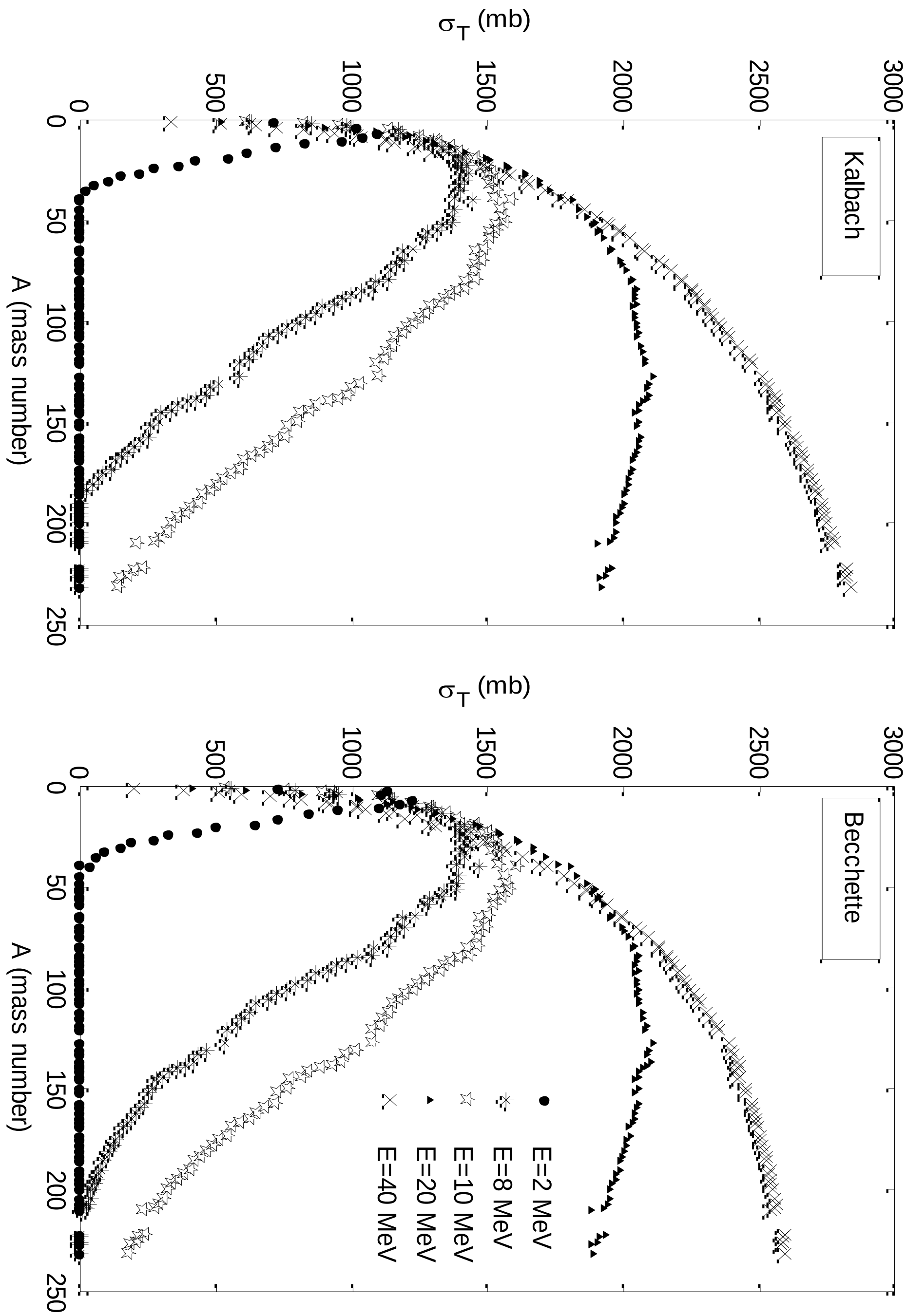

Figure 3. Same as Figure 1 but for incident triton and the optical potentials of Kalbach [7] and Becchette [5] were used.

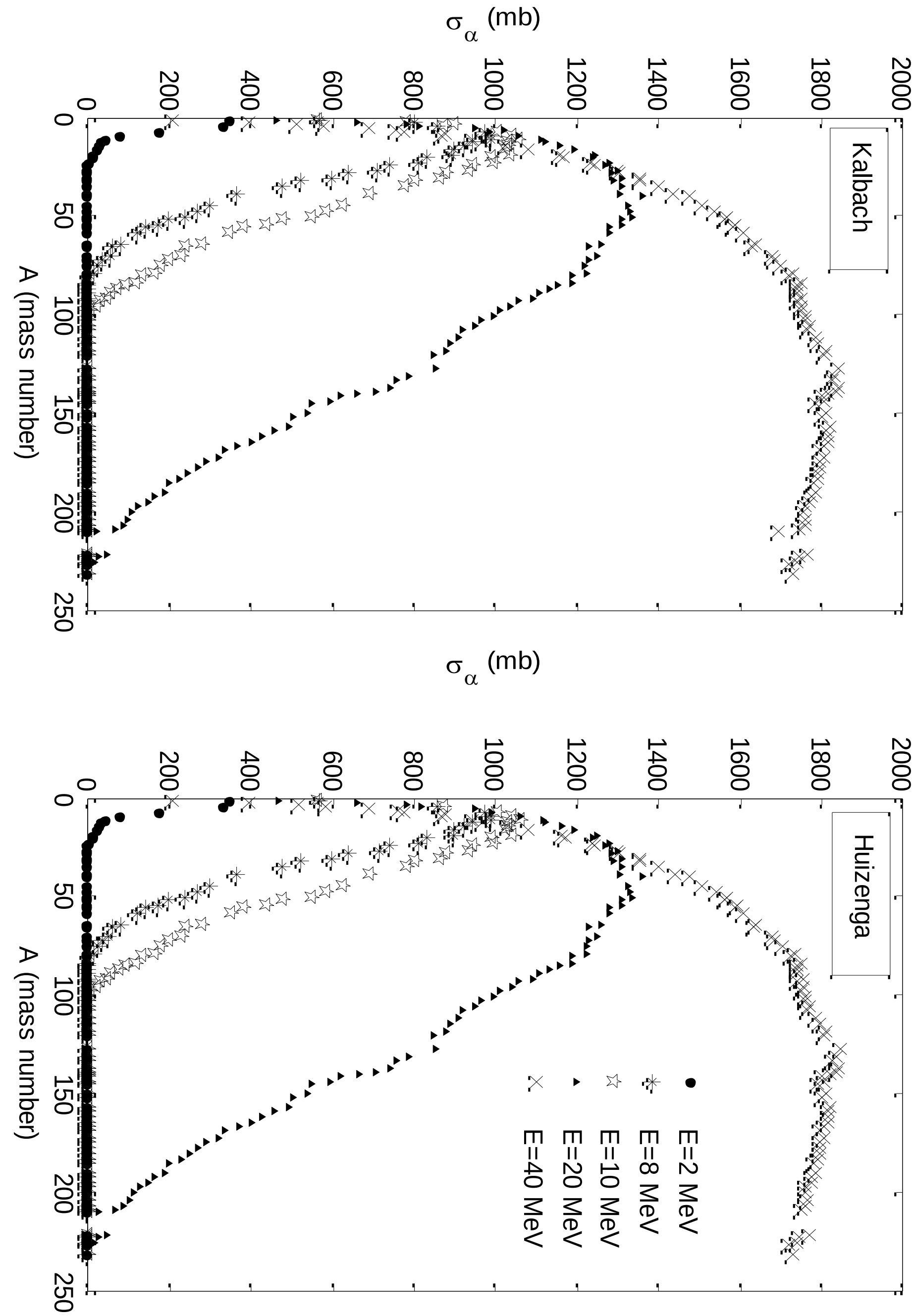

Figure 4. Same as Figure 1 but for incident alpha particle and the optical potentials of Kalbach [7] and Huizenga [11] were used.

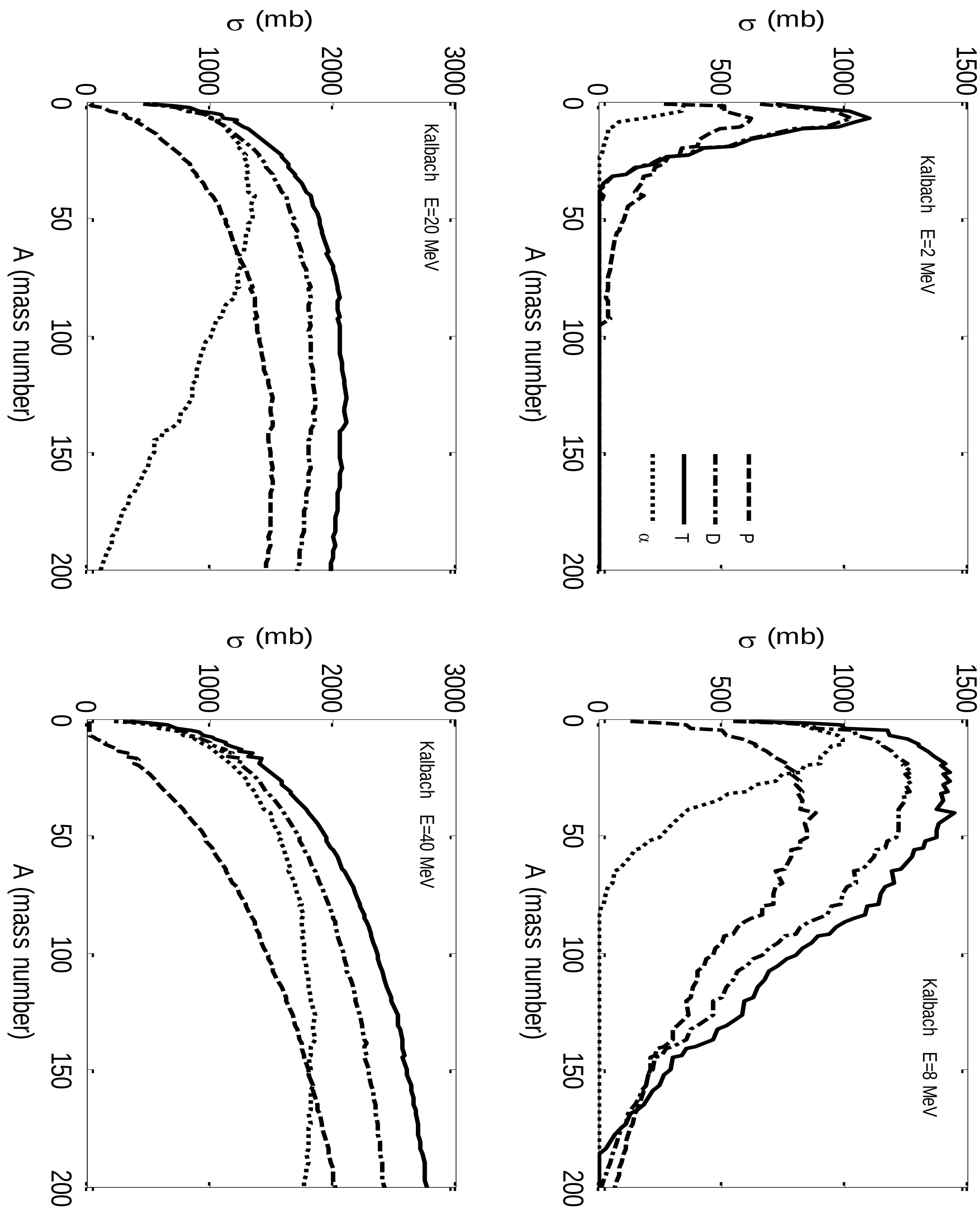

Figure 5. The inverse reaction cross section using Kalbach optical potentials as a function of target mass for incident proton, deuteron, triton, and alpha particle using different incident particle energies.

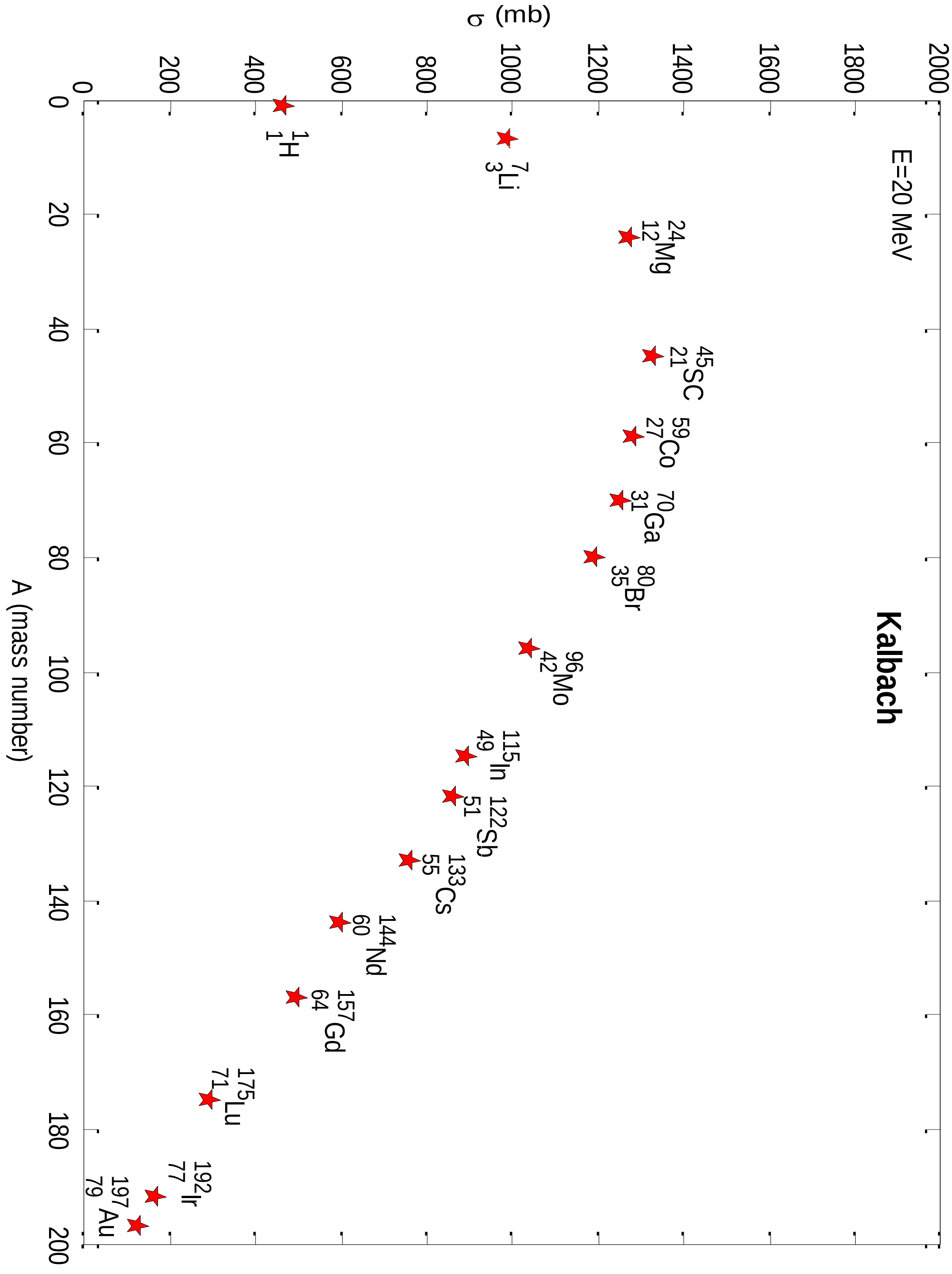

Figure 6. The inverse reaction cross section using Kalbach optical potentials for 20 MeV incident alpha particle. The figure indicate 16 of 232 nuclei used in this work.

It is clear that the increasing in the incident particle energy will increase the reaction cross section. Figure (6) is the same as (5) but for 20 MeV incident alpha particle, this figure shows only 16 of 232 nuclei used in this work. These target nuclei were chosen arbitrary to indicate the behavior of the cross section for inverse reaction when 20 MeV alpha particle interact with the target nuclei. It is obvious in the figure that the maximum $\sigma_{\alpha}(\varepsilon)$ is when α −particle incident on ${}^{46}_{21}Sc$ and then it will start to decrease, since the effect of Coulomb barrier reduces the probability of interaction.

It is concluded that there is a large effect of the charged particles Coulomb barrier on the inverse reaction cross section, for this the corrected results for kalbach need to be considered in future calculations for the pre-equilibrium spectrum. When the incident particles have the same atomic number like p, ${}^{2}_{1}H$, ${}^{3}_{1}H$ the cross section for the inverse reaction will be increase as the incident particle energy increases, but the increasing in the atomic number for incident charged particles like ${}^{4}_{2}He$ will cause a major effect on the interaction probability, where the effect of the sub barrier increase and this will cause a reduction in the cross section for the inverse reaction. In case of high mass number nuclei (varies depending on the incident particle energy), there is no interaction between the incident particle and these high mass number nuclei at low incident energies, or in other words there is no probability for interacting between the low energy incident charged particles and a high mass number nuclei.

References

[1] Dostrovsky I., Frankel Z., and Friedlander G., 1959, *Phys. Rev.* 116, p. 683.

[2] Feshbach H., and V. Weisskopf, 1949, *Phys. Rev.* 76, p. 1550.

[3] Shapiro M. M., 1953, *Phys. Rev.* 90, p. 171.

[4] Mani G. S., Melkanoff M. A., and Iori I., 1963, Centre d'Etudes Nucléaires de Saclay report CEA 2380.

[5] Becchetti F. D., and Greenlees G.W., 1969, *Phys. Rev.* 182, p. 1190.

[6] Chatterjee A., Murthy K. H. N., and Gupta S. K., 1981, *Pramana* 16, p. 391.

[7] Kalbach C., 2007. Users Manual for PRECO-2006, Exciton Model Preequilibrium Nuclear Reaction Code with Direct Reactions. Triangle Universities Nuclear Laboratory, Duke University.

[8] Menet J. J. H., Gross E. E., Malanify J. J., and Zucker A., 1971, *Phys. Rev.* C4, p. 1114.

[9] Schwandt P., and Haeberli W., 1969, *Nucl. Phys.* A123, p. 401.

[10] Becchetti F. D., and Greenlees G. W., 1971, Polarization phenomena in nuclear reactions (eds H H Bars- chall and W Haeberli) (Univ. of Wisconsin Press) p. 682.

[11] Huizenga J. R. and Igo G. T., 1961, Argonne National Laboratory Report No. ANL-6373.

(Received 22 October 2015; accepted 07 November 2015)